Acta Crystallographica Section D
Biological Crystallography
ISSN 0907-4449

Structure–activity correlations of variant forms of the B pentamer of *Escherichia coli* type II heat-labile enterotoxin LT-IIb with Toll-like receptor 2 binding

Vivian Cody,[a,b]* Jim Pace,[a] Hesham F. Nawar,[c]‡ Natalie King-Lyons,[c] Shuang Liang,[d] Terry D. Connell[c] and George Hajishengallis[e]

[a]Structural Biology Department, Hauptman–Woodward Medical Research Institute, 700 Ellicott Street, Buffalo, NY 14203, USA, [b]Structural Biology Department, School of Medicine and Biomedical Sciences, University at Buffalo, 700 Ellicott Street, Buffalo, NY 14203, USA, [c]Department of Microbiology and Immunology and The Witebsky Center for Microbial Pathogenesis and Immunology, School of Medicine and Biomedical Sciences, University at Buffalo, 3435 Main Street, Buffalo, NY 14214, USA, [d]Center for Oral Health and Systemic Disease, University of Louisville School of Dentistry, Louisville, KY 40292, USA, and [e]Department of Microbiology, University of Pennsylvania School of Dental Medicine, Philadelphia, PA 19104-6030, USA

‡ Current address: Division of Bacterial, Allergenic and Parasitic Products, Center for Biologics Evaluations and Research, Food and Drug Administration, Bethesda, MD 20892, USA.

Correspondence e-mail: cody@hwi.buffalo.edu

Received 3 July 2012
Accepted 11 September 2012

PDB References:
LT-IIb-B_5(S74D), 4fnf;
LT-IIb-B_5(T13I), 4fo2;
LT-IIb-B_5(S74A), 4fp5

The pentameric B subunit of the type II heat-labile enterotoxin of *Escherichia coli* (LT-IIb-B_5) is a potent signaling molecule capable of modulating innate immune responses. It has previously been shown that LT-IIb-B_5, but not the LT-IIb-B_5 Ser74Asp variant [LT-IIb-B_5(S74D)], activates Toll-like receptor (TLR2) signaling in macrophages. Consistent with this, the LT-IIb-B_5(S74D) variant failed to bind TLR2, in contrast to LT-IIb-B_5 and the LT-IIb-B_5 Thr13Ile [LT-IIb-B_5(T13I)] and LT-IIb-B_5 Ser74Ala [LT-IIb-B_5(S74A)] variants, which displayed the highest binding activity to TLR2. Crystal structures of the Ser74Asp, Ser74Ala and Thr13Ile variants of LT-IIb-B_5 have been determined to 1.90, 1.40 and 1.90 Å resolution, respectively. The structural data for the Ser74Asp variant reveal that the carboxylate side chain points into the pore, thereby reducing the pore size compared with that of the wild-type or the Ser74Ala variant B pentamer. On the basis of these crystallographic data, the reduced TLR2-binding affinity of the LT-IIb-B_5(S74D) variant may be the result of the pore of the pentamer being closed. On the other hand, the explanation for the enhanced TLR2-binding activity of the LT-IIb-B_5(S74A) variant is more complex as its activity is greater than that of the wild-type B pentamer, which also has an open pore as the Ser74 side chain points away from the pore opening. Data for the LT-IIb-B_5(T13I) variant show that four of the five variant side chains point to the outside surface of the pentamer and one residue points inside. These data are consistent with the lack of binding of the LT-IIb-B_5(T13I) variant to GD1a ganglioside.

1. Introduction

The type II heat-labile enterotoxin of *Escherichia coli* (LT-IIb) is a potent immunologic adjuvant that is closely related in structure and function to cholera toxin (CT) and LT-I, the type I heat-labile enterotoxins of *Vibrio cholerae* and *E. coli*, respectively (Nawar *et al.*, 2005; Liang, Hosur, Lu *et al.*, 2009; Liang, Hosur, Nawar *et al.*, 2009; Berenson *et al.*, 2010; da Hora *et al.*, 2011). Both type I and type II enterotoxins have a similar A_1B_5 oligomeric structure in which the enzymatically active and toxic A subunit is noncovalently inserted into the pore of the doughnut-shaped B pentameric subunit (van den Akker *et al.*, 1996; Gill *et al.*, 1981). The major receptors for type I and type II heat-labile enterotoxins are gangliosides that are components of the eukaryotic plasma membrane (Sonnino *et al.*, 1986). LT-IIb binds with high affinity to ganglioside GD1a and has lower affinities for several other gangliosides (Nawar *et al.*, 2010) and Toll-like receptor (TLR2; Hajishengallis *et al.*, 2005). The membrane-facing side of the B pentamer, the so-called 'lower' region of the B pentamer of

LT-IIb, interacts hydrophilically with the oligosaccharide moiety of GD1a, whereas the 'upper' region of the B pentamer pore contains a large hydrophobic surface which interacts hydrophobically with the A2 segment of the A subunit (van den Akker *et al.*, 1996). Mutational data for other residues in the upper pore region of LT-IIb-B_5 that render the surface more hydrophilic (*i.e.* M69E, A70D and L73E) have been shown to inhibit binding to TLR2 and TLR1 (Liang, Hosur, Lu *et al.*, 2009).

The Toll-like receptor (TLR) family is integral to both innate and adaptive immunity for host defense and plays a crucial role in the immune system by recognition of microbial lipids, carbohydrates, nucleic acids and proteins (Hoffmann *et al.*, 1999; Kopp & Medzhitov, 1999; Anderson, 2000; Kang & Lee, 2011). TLRs are type I transmembrane glycoproteins with a single transmembrane domain and a conserved intracellular domain that share a conserved cytoplasmic domain called the Toll/interleukin-1 receptor (TIR) domain. To date, ten human and 12 mouse TLRs have been identified (Kang & Lee, 2011). Analysis of TLRs reveals that they oligomerize in specific ways. For example, TLR2 is unique in that it can form heterodimers with other TLRs, specifically TLR1 and TLR6, that can bind to lipopeptides from bacterial membranes. Similarly, TLR4 forms heterodimers with MD-2 that are activated by lipopolysaccharides from Gram-negative bacteria (Kang & Lee, 2011).

Structural data have been reported for five extracellular domains of TLRs in complex with agonist or antagonist ligands (Liu *et al.*, 2008; Jin *et al.*, 2007; Kang *et al.*, 2009; Park *et al.*, 2009; Kim *et al.*, 2007; Ohto *et al.*, 2007). These data reveal that the TLRs are rigid and that ligand binding causes only local perturbations. A unique property of these structures is the observation that TLR2, TLR3 and TLR4 use different regions of the receptor for ligand binding (Kang & Lee, 2011). Despite these binding differences, the overall shape of these complexes is similar. This is exemplified by the 'M-shaped' heterodimeric structure of TLR2–TLR1 in complex with Pam_3CSK_4 (Jin *et al.*, 2007).

Recent data have shown that the pentameric B subunit of LT-IIb enterotoxin (LT-IIb-B_5) activates Toll-like receptor (TLR2) signaling in macrophages, in contrast to the Ser74Asp variant of LT-IIb-B_5 [LT-IIb-B_5(S74D)], which further fails to activate bone marrow-derived dendritic cells, while maintaining full GD1a ganglioside-binding capacity (Liang, Hosur, Lu *et al.*, 2009).

The LT-IIb-B_5(T13I) variant retains binding activity for T cells, B cells and macrophages (Nawar *et al.*, 2005; Liang *et al.*, 2007). These data suggest that this immune-stimulatory variant interacts with one or more lymphoid cell receptors. The LT-IIb-B_5(T13I) variant also showed no detectable binding affinity for the gangliosides GD1a, GM2 or GM3; however, it does retain mucosal adjuvant activity (Hajishengallis *et al.*, 2005; Berenson *et al.*, 2010). These data showed weaker binding of GD1a to the LT-IIb-B_5(T13I) variant than to wild-type LT-IIb-B_5 and suggested that the biological activity of the LT-IIb-B_5(T13I) variant is mediated through binding to glycosphingolipid receptors that are distinct from those of the wild-type enterotoxin (Berenson *et al.*, 2010). These studies suggested that the LT-IIb-B_5(T13I) variant results in the preferential binding of NeuGc gangliosides compared with the nearly equal preference of the wild-type toxin for both NeuGc and NeuAc gangliosides (Berenson *et al.*, 2010).

The crystal structures of both cholera toxin (CT) and heat-labile enterotoxin (LT) have been extensively studied as the holo toxin and as the B pentamer complexed with various carbohydrate ligands (Fan *et al.*, 2001; Holmner *et al.*, 2004, 2007, 2011; Merritt & Hol, 1995; Minke *et al.*, 2000; Pickens *et al.*, 2002; van den Akker *et al.*, 1996, 1997). These data reveal a high degree of similarity in the fold of the pentameric units of these two structurally and functionally related enterotoxins.

In order to understand the function of the S74A, S74D and T13I variants of *E. coli* LT-IIb-B_5, their crystal structures were determined and are reported here. These structures are compared with those of the native LT-IIb-B_5 protein (PDB entry 1qb5; E. A. Merritt, F. van den Akker, T. D. Connell, R. K. Holmes & W. G. J. Hol, unpublished work) and the A_1B_5 holo toxin (van den Akker *et al.*, 1996). Moreover, using direct TLR2-binding assays, we compared the TLR2 binding of the LT-IIb-B_5(S74D) variant, another upper-region variant (S74A) and a lower-region variant (T13I), and related their binding activities to their structures.

2. Methods

2.1. Production and purification of mutant LT-IIb-B_5 and Toll-like receptor

Recombinant B subunits of LT-IIb were produced and purified as previously described (Nawar *et al.*, 2005; Liang, Hosur, Lu *et al.*, 2009; Liang, Hosur, Nawar *et al.*, 2009). In brief, pHN16.2, pHN19 and pHN50 encoding the wild-type, LT-IIb-B_5(T13I), LT-IIb-B_5(S74D) or LT-IIb-B_5(S74A) mutant His-tagged B pentamer were expressed in *E. coli* DH5αF′Kan cells (Life Technologies, Gaithersburg, Maryland, USA) after induction with isopropyl β-D-1-thiogalactopyranoside. Pentamers were purified by nickel (or cobalt) affinity chromatography followed by gel-filtration chromatography (Sephacryl S-100; Pharmacia, Piscataway, New Jersey, USA). The purity of the pentamers was confirmed by SDS–PAGE after staining with Coomassie Brilliant Blue and silver (data not shown).

Recombinant Toll-like receptors TLR1 and TLR2 were produced and purified as described by Jin *et al.* (2007) and as described in the Supplementary Material.[1]

2.2. TLR2-binding assay

The binding of ligands to plate-immobilized TLRs was assessed as described previously (Liang *et al.*, 2007). Briefly, 96-well microtiter wells were coated overnight at 277 K with 20 $\mu g\ ml^{-1}$ recombinant mouse or human TLR2 (R&D Systems). After blocking nonspecific binding sites with

[1] Supplementary material has been deposited in the IUCr electronic archive (Reference: MH5069). Services for accessing this material are described at the back of the journal.

Table 1
Crystal properties and refinement parameters for the enterotoxin variants LT-IIb-B_5(S74D), LT-IIb-B_5(S74A) and LT-IIb-B_5(T13I).

Values in parentheses are for the highest resolution shell.

Mutant	Ser74Asp	Ser74Ala	Thr13Ile
PDB code	4fnf	4fp5	4fo2
Space group	*C*2	$P2_12_12_1$	*C*2
Unit-cell parameters			
a (Å)	138.5	48.4	119.3
b (Å)	70.6	67.6	120.0
c (Å)	60.9	155.6	142.5
β (°)	114.4	90.0	90.1
Z	2	1	4
Beamline	SSRL 9-2	SSRL 9-2	SSRL 11-1
Resolution (Å)	45.64–1.60 (1.69–1.60)	48.41–1.40 (1.50–1.40)	45.79–1.50 (1.58–1.50)
Wavelength (Å)	0.979	0.979	0.979
$R_{\rm merge}$†	0.10 (0.74)	0.065 (0.33)	0.058 (0.92)
$R_{\rm p.i.m.}$	0.06 (0.48)	0.029 (0.14)	0.035 (0.79)
Completeness (%)	98.6 (100)	99.8 (100)	98.1 (87.6)
Observed reflections	216828 (31294)	615754 (88505)	1133937 (106093)
Unique reflections	69593 (10306)	101201 (14647)	313200 (40708)
$\langle I/\sigma(I)\rangle$	6.2 (1.3)	14.1 (4.2)	10.8 (0.9)
Multiplicity	3.1 (3.0)	6.1 (6.0)	3.6 (2.6)
Refinement and model quality			
Resolution range (Å)	30.8–1.90 (2.00–1.90)	41.1–1.40 (1.48–1.40)	45.8–1.90 (2.00–1.90)
No. of reflections	78189	96076	157386
R factor‡ (%)	21.3	18.1	18.9
$R_{\rm free}$§ (%)	26.3	21.2	23.7
Total protein atoms	8579	4166	15604
Total water atoms	959	391	591
Average *B* factor (Å^2)	23.4	15.6	24.8
R.m.s. deviation from ideal			
Bond lengths (Å)	0.03	0.03	0.02
Bond angles (°)	2.38	2.40	2.46
Luzzati coordinate error (Å)	0.28	0.15	0.21
Ramachandran plot			
Most favored regions (%)	98.3	99.2	97.4
Additional allowed regions (%)	0.7	0.6	1.8
Generously allowed regions (%)	0.9	0.2	0.8
Disallowed regions (%)	0.0	0.0	0.0

† $R_{\rm merge} = \sum_{hkl}\sum_i |I_i(hkl) - \langle I(hkl)\rangle| / \sum_{hkl}\sum_i I_i(hkl)$, where $\langle I(hkl)\rangle$ is the mean intensity of a set of equivalent reflections. ‡ *R* factor $= \sum_{hkl} \big||F_{\rm obs}| - |F_{\rm calc}|\big| / \sum_{hkl} |F_{\rm obs}|$, where $F_{\rm obs}$ and $F_{\rm calc}$ are observed and calculated structure-factor amplitudes. § $R_{\rm free}$ was calculated as for the *R* factor but for a random 5% subset of all reflections that were exluded from refinement.

5%(*w*/*v*) BSA, 10 µg ml^{-1} wild-type or mutant LT-IIb-B_5 was incubated in PBS containing 5% BSA. Bound protein was detected calorimetrically using rabbit IgG anti-LT-IIb Ab followed by peroxidase-conjugated goat anti-rabbit IgG (adsorbed against human or mouse IgG).

2.3. Crystallization of the LT-IIb-B_5(S74D) variant

The protein was concentrated to 7.5 mg ml^{-1} in water. Crystallization screening using the HWI 1536-well robot resulted in 11 hits from the high-throughput screen (Luft *et al.*, 2003). However, only two of these conditions reproduced crystals when set up on a larger scale. Crystals were grown in a 287 K incubation room by the microbatch-under-oil method using a 1:1 ratio of protein solution to reservoir solution (20% PEG 400, 100 m*M* K_2HPO_4, 100 m*M* sodium acetate pH 5.0) in a 4 µl droplet. Glycerol was added to 24%(*v*/*v*) for cryoprotection. Crystals grew over several days and were monoclinic, belonging to space group *C*2 and diffracting to 1.6 Å resolution.

2.4. Crystallization of the LT-IIb-B_5(S74A) variant

The protein was concentrated to 3.2 mg ml^{-1} in 100 m*M* Tris pH 8.0. Crystallization screens were set up using the hanging-drop method with 2 µl protein solution and 2 µl reservoir solution and were placed in a 287 K incubation room. Crystals appeared within several minutes and continued to grow. The crystals used for data collection were grown in condition No. 88 of The PACT Suite from Qiagen (100 m*M* bis-Tris propane pH 8.5, 20% PEG 3350, 200 m*M* KSCN) and were orthorhombic; they belonged to space group $P2_12_12_1$ and diffracted to 1.40 Å resolution. The crystals were cryoprotected with Paratone-N oil (Hampton Research, California, USA).

2.5. Crystallization of the LT-IIb-B_5(T13I) variant

The protein was concentrated to 10.0 mg ml^{-1} in water. Crystallization screening using the HWI 1536-well robot resulted in four hits, from which two sets of conditions resulted in good diffraction-quality crystals when set up using the microbatch-under-oil method (Luft *et al.*, 2003). Crystals were grown in a 293 K incubation room by the microbatch-under-oil method using a 1:1 ratio of protein solution to reservoir solution in a 6 µl droplet that contained 50 m*M* Tris pH 7.5, 100 m*M* NaCl and a reservoir solution consisting of 60% Tacsimate (Hampton Research Index Screen condition No. 29). Crystals grew over several days and were monoclinic, belonging to space group *C*2 and diffracting to 1.5 Å resolution. Glycerol was added to 25%(*v*/*v*) for cryoprotection.

2.6. Data collection, structure determination and refinement

Data for crystals of the LT-IIb-B_5(S74D) and LT-IIb-B_5(S74A) variants were collected at cryogenic temperature on beamline 9-2 at the Stanford Synchrotron Radiation Lightsource (SSRL) using the remote-access system (McPhillips *et al.*, 2002; Cohen *et al.*, 2002; González *et al.*, 2008), while data for the LT-IIb-B_5(T13I) mutant were collected on beamline 11-1 at SSRL. A lower resolution data set for the LT-IIb-B_5(S74D) variant was also collected to 1.9 Å resolution on a Rigaku Saturn 944+ CCD AFC111 detector at HWI. All data

were processed with *MOSFLM* (Leslie & Powell, 2007) and scaled with *SCALA* (Evans, 2006). The unit-cell parameters and diffraction statistics are given in Table 1.

The structures were solved by the molecular-replacement method using the coordinates of wild-type LT-IIb-B_5 (PDB entry 1qb5; E. A. Merritt, F. van den Akker, T. D. Connell, R. K. Holmes & W. G. J. Hol, unpublished work) as a model with *MOLREP* (Vagin & Teplyakov, 2010) as implemented in the *CCP*4 suite of programs (Winn *et al.*, 2011). Inspection of the resulting electron-density maps was performed using the program *Coot* (Emsley *et al.*, 2010) running on a Mac G5 workstation and revealed density for two B pentamers in the asymmetric unit of the LT-IIb-B_5(S74D) mutant lattice, four B pentamers in the asymmetric unit of the LT-IIb-B_5(T13I) variant and one pentamer in the LT-IIb-B_5(S74A) variant. To monitor the refinement, a random subset (5%) of all reflections was set aside for calculation of $R_{\rm free}$. Electron density was not observed for the C-terminal Glu99 residue in all individual subunits of the B pentamer in all of the structures. The final cycles of refinement were carried out using the program *REFMAC*5 (Murshudov *et al.*, 2011) as implemented in *CCP*4 (Winn *et al.*, 2011). Between least-squares minimizations, the structures were manually adjusted to fit the observed electron density. Difference electron-density maps were monitored for improvement during the refinement based on high-resolution cutoffs, particularly in those data sets with high $R_{\rm merge}$ in the highest resolution shells (Table 1). New research tools that help in selecting resolution-cutoff criteria indicate that high-resolution data with high $R_{\rm merge}$ can be used provided that their inclusion improves the refinement (Karplus & Diederichs, 2012). The Ramachandran conformational parameters generated by *RAMPAGE* (Lovell *et al.*, 2002) for the final models in the last cycles of refinement showed that more than 97% of the residues in these structures have the most favored conformation and none are in disallowed regions (Table 1). Coordinates for these structures have been deposited in the Protein Data Bank (Table 1). Superpositions were computed with the *SSM* function (Krissinel & Henrick, 2004) in *Coot* (Emsley *et al.*, 2010) using the same reference structure. Figures were prepared using the modeling program *PyMOL* (DeLano, 2002).

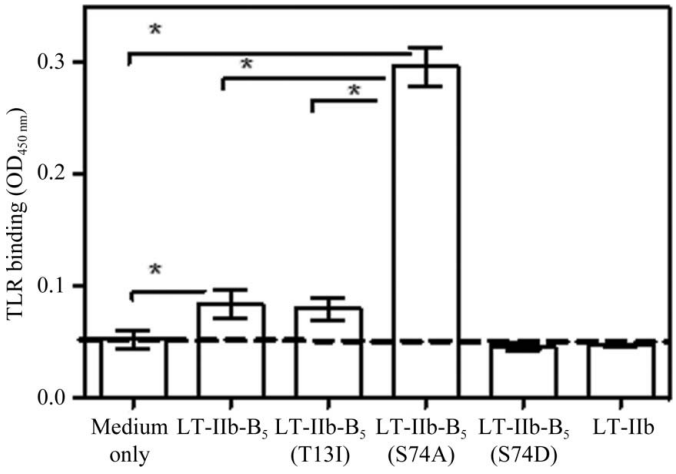

Figure 1
Substitutions with hydrophobic residues in the upper region of LT-IIb-B_5 enhance binding to TLR2. Binding of wild-type (WT) LT-IIb-B_5, the hydrophobic point variant LT-IIb-B_5(S74A) or the hydrophilic variant LT-IIb-B_5(S74D) was determined in microtiter wells coated with mouse TLR2. The LT-IIb holotoxin was used as a negative control in the TLR2-binding assays. All ligands were used at 10 μg ml^{-1}, and bound protein was detected colorimetrically after probing with anti-LT-IIb Ab followed by addition of peroxidase-conjugated secondary Abs. Data are mean ± s.d. (n = 3) from one of three independent sets of experiments that yielded similar results.

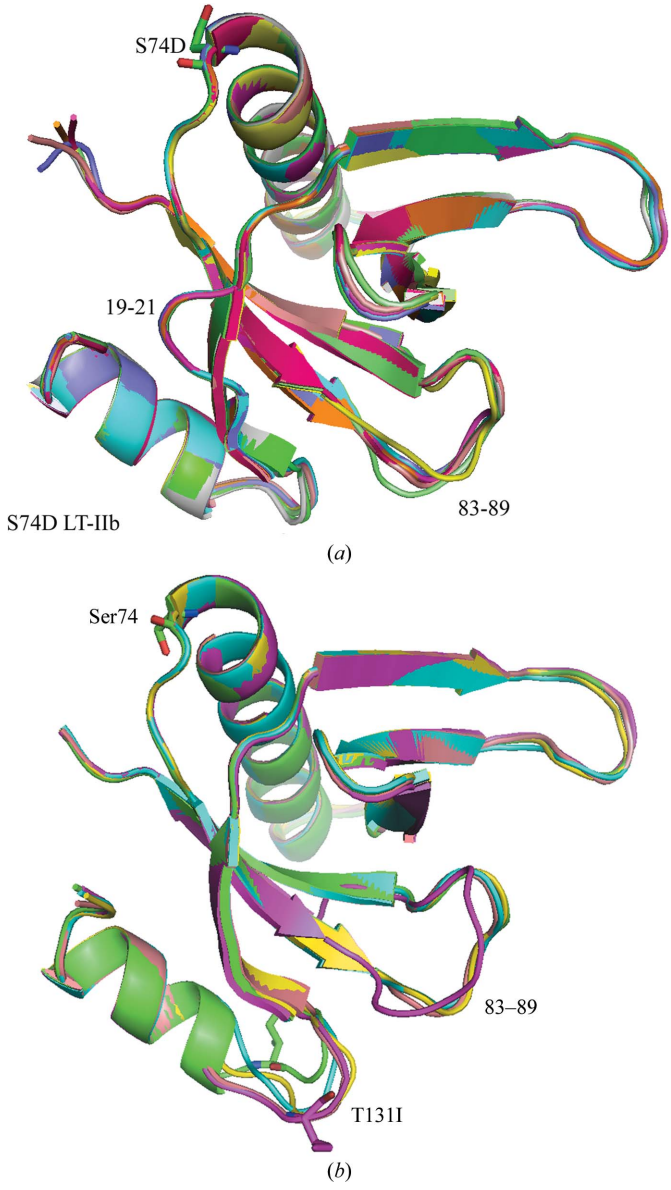

Figure 2
(*a*) Superposition of the individual B-pentamer subunits (colored separately: *D*, green; *E*, cyan; *F*, violet; *G*, yellow; *H*, pink) of the LT-IIb-B_5(S74D) variant. These data show disorder in the conformation of the loop near residues 83–89 among the individual subunits, as well as a flexible region near residues 19–21 of two of the individual subunits of the B pentamer. (*b*) Similar comparison for the LT-II-B_5(T13I) variant. Note the absence of the disordered region near residues 19–21.

3. Results

3.1. TLR2 binding by LT-IIb-B_5 and variants

Having identified specific LT-IIb-B_5 residues (Met69, Ala70, Leu73 and Ser74) which are critical for TLR2 binding through hydrophobic interactions (Liang, Hosur, Lu *et al.*, 2009; Liang, Hosur, Nawar *et al.*, 2009), we constructed an 'enhanced hydrophobic' version of LT-IIb-B_5, LT-IIb-B_5(S74A), under the hypothesis that this mutant may interact more potently with TLR2. In contrast, the 'enhanced hydrophilic' LT-IIb-B_5(S74D) variant, which fails to activate TLR2 signaling (Liang, Hosur, Lu *et al.*, 2009), would be used as a negative control in the TLR2-binding assay together with the LT-IIb holotoxin, in which the A subunit blocks the TLR2 interactive domain in the 'upper region' of the B pentameric subunit (Liang, Hosur, Lu *et al.*, 2009; Liang, Hosur, Nawar *et al.*, 2009). In contrast, the Thr13Ile variant involves the 'lower region' of the B pentamer, so we hypothesized that its TLR2-binding activity would not be affected positively or negatively. Our data fully supported these hypotheses, since the LT-IIb-B_5(S74A) variant displayed about sixfold stronger binding to TLR2 than the wild-type LT-IIb-B_5 or the LT-IIb-B_5(T13I) variant, which bind comparably to the wild-type B pentamer (Fig. 1). In contrast, the LT-IIb-B_5(S74D) variant and the LT-IIb holotoxin failed to bind TLR2 (Fig. 1).

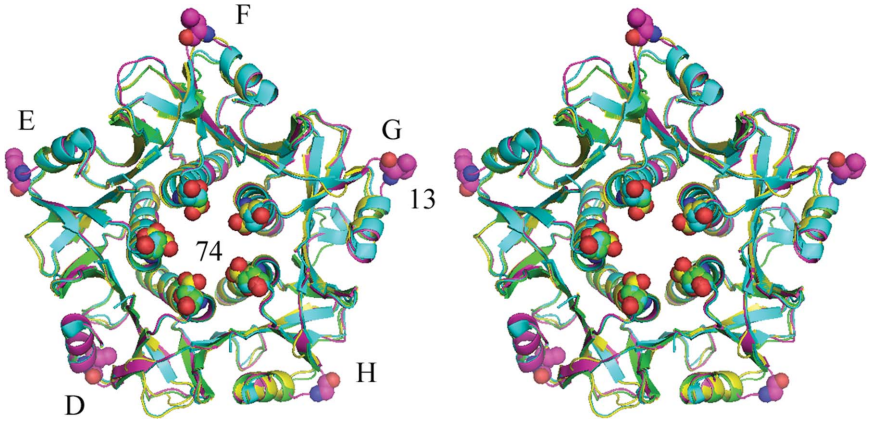

Figure 3
Superposition of the LT-II-B_5(S74A) variant (green), with residue 74 shown as a space-filling representation, on the wild-type protein (cyan; van den Akker *et al.*, 1996), the LT-IIb-B_5(S74D) variant (yellow) and the LT-IIb-B_5(T13I) variant (violet), with residue 13 shown as a space-filling representation. The mutations at positions 13, 74 and 74 are shown as space-filling spheres. The individual subunits of the B pentamer are labeled *D*–*H*.

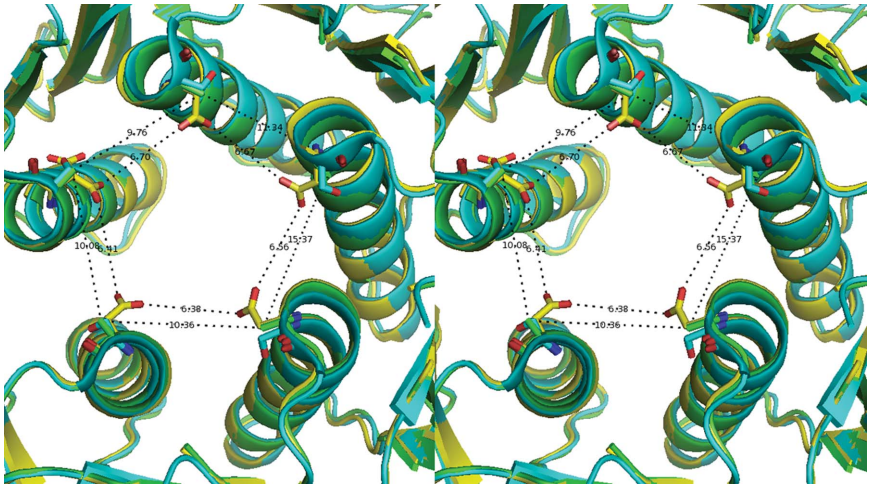

Figure 4
Stereo comparison of the Ser74Ala (green), Ser74Asp (yellow) and wild-type (Ser74; cyan; van den Akker *et al.*, 1996) variants of LT-II-B_5. The contact distances between the Asp74 carboxyl O atoms are shown. Also included are the contact distances from the Ala74 methyl group. The effect of the Ser74Asp mutant is to reduce the pore opening in this variant compared with that in the Ser74Ala variant.

3.2. Crystal structures

Each of the five 99-residue individual subunits of the LT-IIb-B_5 pentamer contains a five-stranded antiparallel β-sheet and two α-helices that assemble to form a central pore with a diameter of 10–18 Å (van den Akker *et al.*, 1996). There is a disulfide bond between Cys10 and Cys81 in each monomer. Few differences are observed between the individual subunits of the B pentamer. The structural data indicate flexible loop regions encompassing residues 83–89 in all individual subunits that differ from the native pentamer (Fig. 2). The C-terminal Glu99 residue is disordered in each of the B subunits and was not included in the refined models.

Crystallization screening using the HWI 1536-well robot (Luft *et al.*, 2003) produced hits from conditions that varied over a wide range of pH values and precipitating agents and differed from those reported for native LT-IIb-B_5 (van den Akker *et al.*, 1996). Two of the variant structures revealed multiple copies of the B pentamer in the asymmetric unit of the crystal lattice (Table 1).

3.3. Ser74Asp and Ser74Ala variants of LT-IIb-B_5

Structural data for the LT-IIb-B_5(S74D) variant shows that there are two pentamers in the asymmetric unit of the *C*2 crystal lattice (Table 1). The carboxylate of Asp74 points into the pore of the pentamer and its conformation is such that it is in the opposite direction to that observed for the Ser74 hydroxyl in the native structure (van den Akker *et al.*, 1996; Fig. 3). Asp74 also has two alternate conformations in one of the individual subunits of the B pentamer. The structure of the LT-IIb-B_5(S74A) variant is similar to that of the LT-IIb-B_5(S74D) variant; however, there is only one pentamer in the asymmetric unit of the orthorhombic lattice (Table 1), as was observed in the native protein (van den Akker *et al.*, 1996).

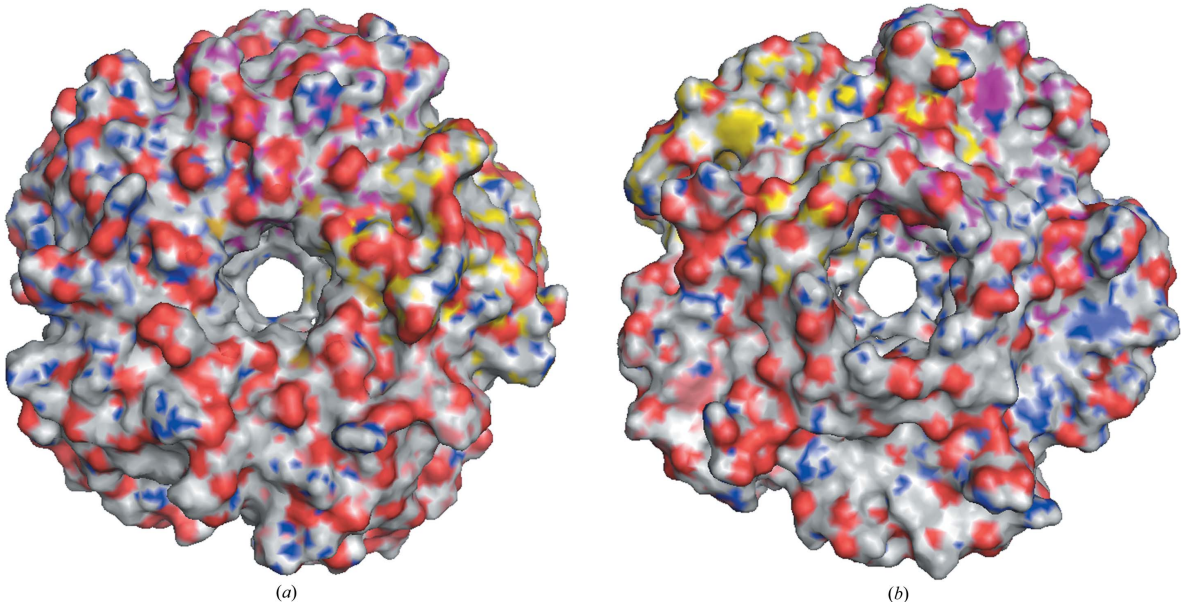

Figure 5
Electrostatic surface representation (red, acidic; blue, basic; yellow, sulfur) of the LT-IIb-B_5(S74A) variant viewed from the top of the pore (*a*) and of the LT-IIb-B_5(S74A) variant viewed from the bottom of the pore (*b*). Note that the pore opening varies in size from the top to the bottom.

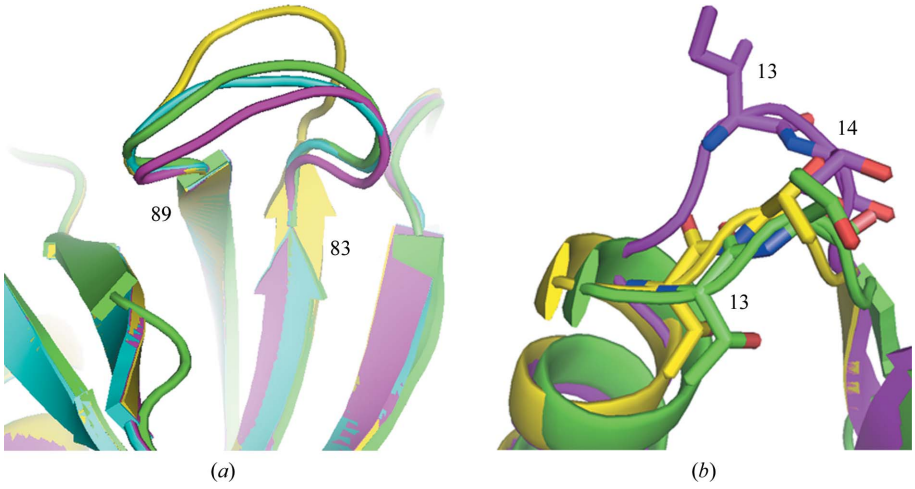

Figure 6
(*a*) Comparison of the flexible loop region between residues 83 and 89 for the Ser74Asp (green), Ser74Ala (cyan) and Thr13Ile (violet) variants and for native LT-II-B_5 (yellow). (*b*) Superposition of residues Ile13–Thr14 from the *G* subunit for the Thr13Ile variant (violet), the Ser74Asp variant (green) and native LT-IIb-B_5 (yellow).

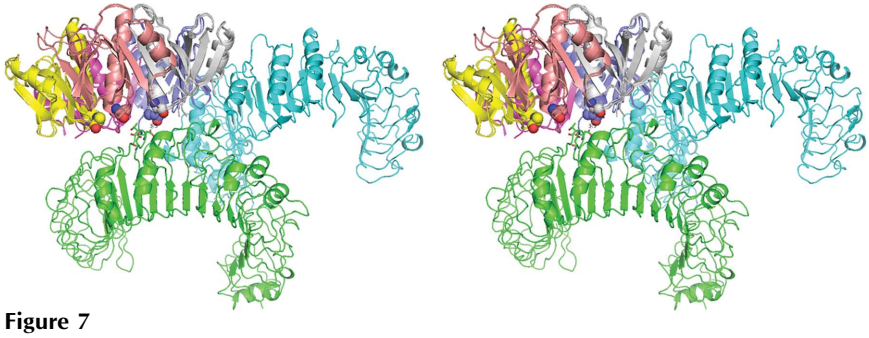

Figure 7
Stereoview of the crystal structure of LT-IIb-B_5(S74A) (multicolored pentamer with Ala74 shown as a space-filling representation) superimposed on wild-type LT-IIb-B_5 modeled into the structure of a TLR2 (green)–TLR1 (cyan) heterodimer complex with residues Asp235 and Asn290 of TLR2 (green) shown as stick representations (Liang, Hosur, Lu *et al.*, 2009).

Comparison of the LT-IIb-B_5(S74D) and LT-IIb-B_5(S74A) variants with native LT-IIb-B_5 reveals that the positioning of the carboxylate moiety of the LT-IIb-B_5(S74D) variant results in a smaller pore opening (6.4–6.7 Å) than in either the native (Ser74) or the Ser74Ala variant (9.8–15.4 Å) (Fig. 4). The net result is that the position of the LT-IIb-B_5(S74D) variant side chain effectively closes the pore opening compared with that of the LT-IIb-B_5(S74A) variant. Comparison of the electrostatic surfaces of LT-IIb-B_5 reveals that the pore size varies from the top to the bottom of the pore, with the surface at the LT-IIb-B_5(S74D) variant face being smaller than the opening at the LT-IIb-B_5(T13I) variant face of the pore (Fig. 5).

3.4. T13I variant of LT-IIb-B_5

Four pentamers are present in the asymmetric unit in the crystal structure of the LT-IIb-B_5(T13I) variant (Table 1). There is flexibility in the conformation of the residues in loop 83–86, as shown for the other variants (Fig. 6*a*). These data also reveal that four of the five individual subunits of the B pentamer have the side chain of Ile13 pointing out from the surface and that the loop encompassing this variant is

more extended than in the native LT-IIb-B_5 structure. The fifth residue points inwards and has a similar loop conformation to that observed for the wild-type structure (Fig. 3). When the Ile13 variant residue is pointing outwards, there is a rearrangement of the strand that involves this variant position and the residues nearby (Fig. 6*b*). In the native structure the hydroxyl of Thr14 is solvent-accessible, as it is in the individual subunit of LT-IIb-B_5(T13I) with Ile13 pointing inward. The hydroxyl group of Thr13 of the native structure is involved in two hydrogen bonds to the carbonyl of Cys10 and the amine of Ala15 (van den Akker *et al.*, 1996). In the LT-IIb-B_5(T13I) variant the side chain of Ile13 in four of the individual subunits of the B pentamer is solvent-accessible and that of Thr14 is not (Fig. 6*b*). This change in conformation is likely to modulate the altered ganglioside interactions observed in the binding patterns of the LT-IIb-B_5(T13I) variant and wild-type LT-IIb-B_5 (Berenson *et al.*, 2010; Nawar *et al.*, 2010).

3.5. Packing arrangement in the LT-IIb-B_5(T13I) variant

Structural results for the LT-IIb-B_5(T13I) variant revealed the presence of eight Na^+ ions in the crystallization medium. The octahedral coordination of these ions helps to stabilize the interactions between the multiple copies of the pentamer in the asymmetric unit of this structure. Details are given in the Supplementary Material.

3.6. Models of TLR2-LT-IIb-B_5 receptor binding

Biochemical data have shown that the pentameric B subunit of LT-IIb-B_5 activates the TLR2–TLR1 heterodimer. These studies indicated that four residues near the Ser74 surface of the pentamer were involved in these interactions, as shown by mutational studies, in which the variants Met69Glu, Ala70Asp, Leu73Glu and Ser74Asp showed reduced binding. Docking analyses of these interactions were carried out that indicated that the B pentamer makes contact with the convex surface of the TLR2 central domain and partially overlaps with that of PAM_3CSK_4 (Liang, Hosur, Lu *et al.*, 2009; Fig. 7). Comparison of the structures of wild-type (Ser74) LT-IIb-B_5 and the LT-IIb-B_5(S74A) variant suggests possible intermolecular contacts between the carbonyl of Ser74 or Ala74 of LT-IIb-B_5 and Asp235 and Asn290 of TLR2 (Figs. 8). Since these contacts involve the backbone carbonyl of Ser74, they would be the same for wild-type LT-IIb-B_5 and the Ser74Ala and Ser74Asp variants.

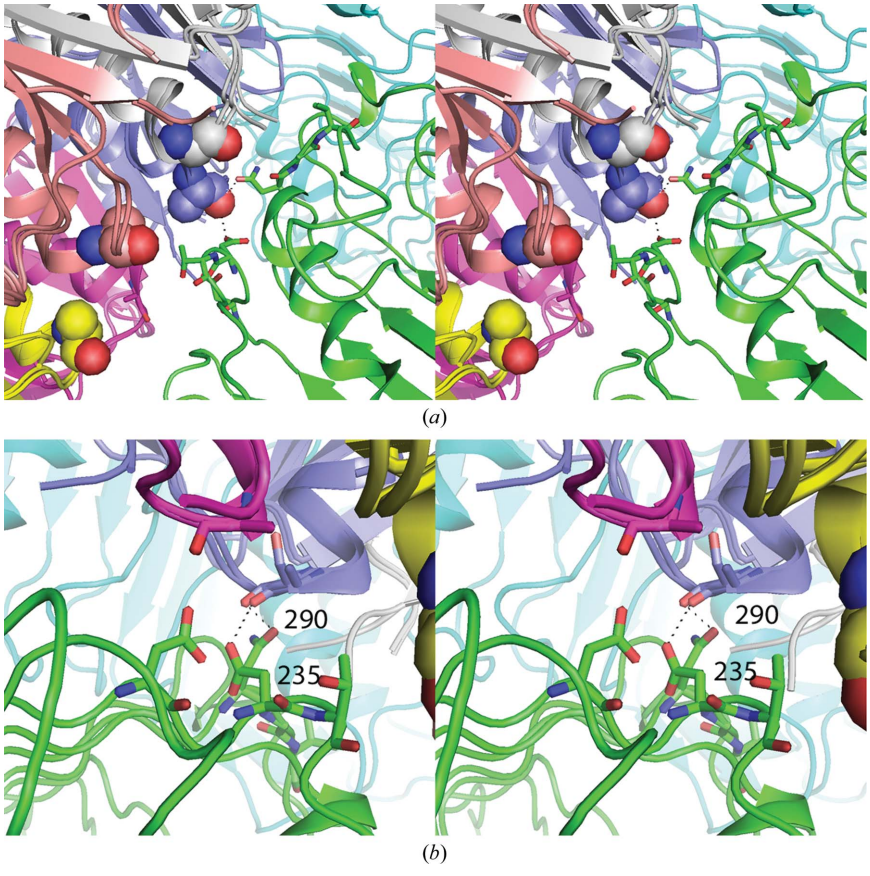

(*a*)

(*b*)

Figure 8
(a) Close-up view of the interaction between LT-IIb-B_5(S74A) (purple; Ala74 shown as a space-filling representation) and Asn290 (stick representation) of TLR2 (green) based on the computational model of the complex of LT-IIb-B_5 with the TLR2–TLR1 heterodimer (green/cyan; Liang, Hosur, Lu *et al.*, 2009). Other individual subunits of the B pentamer are shown in violet and yellow. (*b*) Comparison of the wild type (Ser74) *versus* the Ser74Ala variant (purple stick figures) of LT-IIb-B_5 (other individual subunits are shown in violet/purple/yellow) highlights the interaction of the Ser74 carbonyl group with the side chains of residues Asn290 and Asp235 (stick representations) of TLR2 (green) in the computed complex between LT-IIb-B_5 and the TLR2–TLR1 heterodimer (green/cyan; Liang, Hosur, Lu *et al.*, 2009). Note that the side chain of Ser74 points away from the interface between these two models.

4. Concluding remarks

The data from the crystallographic and TLR2-binding analyses of LT-IIb-B_5(S74A) provide useful insight into the structure–function relationship in the LT-IIb-B_5 molecule. Consistent with previous cellular activation data, the LT-IIb-B_5(S74D) variant failed to bind TLR2, in contrast to wild-type LT-IIb-B_5 and the LT-IIb-B_5(T13I) variant, in which the variant residue is independent and far from the upper region of the B pentamer that interacts with TLR2 (Liang, Hosur, Lu *et al.*, 2009). Strikingly, the LT-IIb-B_5(S74A) variant displayed significantly higher binding to TLR2 than wild-type LT-IIb-B_5. However, an explanation of the enhanced activity of the LT-IIb-B_5(S74A) variant compared with the wild-type B pentamer is not clear as the Ser74 side chain points away from the pore center, thereby presenting a similar hydrophobic profile to the pore center as the LT-IIb-B_5(S74A) variant. Other properties, such as electrostatic character, side-chain

conformational flexibility, hydrophilicity, hydrophobicity, acidic properties or steric effects, may also contribute to TLR2-binding activity. Further structural studies of other Ser74 variants (*i.e.* Thr74, Pro74 and Gly74) would be required to validate these contributions. Also, structural analysis of those variants that make the B pentamer more acidic (*i.e.* Met69Glu, Ala70Asp and Leu73Glu; Liang, Hosur, Lu *et al.*, 2009) would be required to address their contributions to pore opening.

On the basis of these crystallographic analyses, we propose that the reduced TLR2-binding activity of the LT-IIb-B_5(S74D) variant may result from the pore of the pentamer being closed by the carboxylate of the Asp74 side chain, which points into the pore. On the other hand, the reason why the LT-IIb-B_5(S74A) variant shows enhanced TLR2 binding compared with the wild type is more complex than simply being attributable to the pore remaining open, as replacement of the hydroxyl group of the Ser74 side chain in the native structure by the methyl group of the Ala74 side chain would give the same contacts with the TLR2 receptor.

To further understand the binding profiles observed for the LT-IIb-B_5 variants, we have undertaken structural studies of LT-IIb-B_5 with GD1a to validate the binding profiles observed for wild-type LT-IIb-B_5 and the Thr13Ile variant. Preliminary structural analyses are in progress. Crystallization trials of cocrystal complexes of LT-IIb-B_5 with TLR2 and TLR1 are also under way in order to validate the computational models described for the complex of the TLR2–TLR1 heterodimer with LT-IIbB_5 (Liang, Hosur, Lu *et al.*, 2009).

This work was supported in part by grants from NIH: DE015254, DE017138 (GH) and DE13833 (TDC). The support of the beamline staff at SSRL is greatly appreciated. Portions of this research were carried out at the Stanford Synchrotron Radiation Lightsource, a national user facility operated by Stanford University on behalf of the US Department of Energy, Office of Basic Energy Sciences. The SSRL Structural Molecular Biology Program is supported by the Department of Energy, Office of Biological and Environmental Research, by the National Institutes of Health, National Center for Research Resources, Biomedical Technology Program and the National Institute of General Medical Sciences.

References

Akker, F. van den, Pizza, M., Rappuoli, R. & Hol, W. G. J. (1997). *Protein Sci.* **6**, 2650–2654.
Akker, F. van den, Sarfaty, S., Twiddy, E. M., Connell, T. D., Holmes, R. K. & Hol, W. G. J. (1996). *Structure*, **4**, 665–678.
Anderson, K. V. (2000). *Curr. Opin. Immunol.* **12**, 13–19.
Berenson, C. S., Nawar, H. F., Yohe, H. C., Castle, S. A., Ashline, D. J., Reinhold, V. N., Hajishengallis, G. & Connell, T. D. (2010). *Glycobiology*, **20**, 41–54.
Cohen, A. E., Ellis, P. J., Miller, M. D., Deacon, A. M. & Phizackerley, R. P. (2002). *J. Appl. Cryst.* **35**, 720–726.
DeLano, W. L. (2002). *PyMOL*. http://www.pymol.org.
Emsley, P., Lohkamp, B., Scott, W. G. & Cowtan, K. (2010). *Acta Cryst.* D**66**, 486–501.
Evans, P. (2006). *Acta Cryst.* D**62**, 72–82.
Fan, E., Merritt, E. A., Zhang, Z., Pickens, J. C., Roach, C., Ahn, M. & Hol, W. G. J. (2001). *Acta Cryst.* D**57**, 201–212.
Gill, D. M., Clements, J. D., Robertson, D. C. & Finkelstein, R. A. (1981). *Infect. Immun.* **33**, 677–682.
González, A., Moorhead, P., McPhillips, S. E., Song, J., Sharp, K., Taylor, J. R., Adams, P. D., Sauter, N. K. & Soltis, S. M. (2008). *J. Appl. Cryst.* **41**, 176–184.
Hajishengallis, G., Arce, S., Gockel, C. M., Connell, T. D. & Russell, M. W. (2005). *J. Dent. Res.* **84**, 1104–1116.
Hoffmann, J. A., Kafatos, F. C., Janeway, C. A. & Ezekowitz, R. A. (1999). *Science*, **284**, 1313–1318.
Holmner, Å., Askarieh, G., Ökvist, M. & Krengel, U. (2007). *J. Mol. Biol.* **371**, 754–764.
Holmner, Å., Lebens, M., Teneberg, S., Ångström, J., Ökvist, M. & Krengel, U. (2004). *Structure*, **12**, 1655–1667.
Holmner, Å., Mackenzie, A., Ökvist, M., Jansson, L., Lebens, M., Teneberg, S. & Krengel, U. (2011). *J. Mol. Biol.* **406**, 387–402.
da Hora, V. P., Conceição, F. R., Dellagostin, O. A. & Doolan, D. L. (2011). *Vaccine*, **29**, 1538–1544.
Jin, M. S., Kim, S. E., Heo, J. Y., Lee, M. E., Kim, H. M., Paik, S.-G., Lee, H. & Lee, J.-O. (2007). *Cell*, **130**, 1071–1082.
Kang, J. Y. & Lee, J.-O. (2011). *Annu. Rev. Biochem.* **80**, 917–941.
Kang, J. Y., Nan, X., Jin, M. S., Youn, S.-J., Ryu, Y. H., Mah, S., Han, S. H., Lee, H., Paik, S.-G. & Lee, J.-O. (2009). *Immunity*, **31**, 873–884.
Karplus, P. A. & Diederichs, K. (2012). *Science*, **336**, 1030–1033.
Kim, H. M., Park, B. S., Kim, J.-I., Kim, S. E., Lee, J., Oh, S. C., Enkhbayar, P., Matsushima, N., Lee, H., Yoo, O. J. & Lee, J.-O. (2007). *Cell*, **130**, 906–917.
Kopp, E. B. & Medzhitov, R. (1999). *Curr. Opin. Immunol.* **11**, 13–18.
Krissinel, E. & Henrick, K. (2004). *Acta Cryst.* D**60**, 2256–2268.
Leslie, A. G. W. & Powell, H. R. (2007). *Evolving Methods for Macromolecular Crystallography*, edited by R. J. Read & J. L. Sussman, pp. 41–51. Dordrecht: Springer.
Liang, S., Hosur, K. B., Lu, S., Nawar, H. F., Weber, B. R., Tapping, R. I., Connell, T. D. & Hajishengallis, G. (2009). *J. Immunol.* **182**, 2978–2985.
Liang, S., Hosur, K. B., Nawar, H. F., Russell, M. W., Connell, T. D. & Hajishengallis, G. (2009). *Vaccine*, **27**, 4302–4308.
Liang, S., Wang, M., Tapping, R. I., Stepensky, V., Nawar, H. F., Triantafilou, M., Triantafilou, K., Connell, T. D. & Hajishengallis, G. (2007). *J. Biol. Chem.* **282**, 7532–7542.
Liu, L., Botos, I., Wang, Y., Leonard, J. N., Shiloach, J., Segal, D. M. & Davies, D. R. (2008). *Science*, **320**, 379–381.
Lovell, S. C., Davis, I. W., Arendell, W. B. III, de Baker, P. I. W., Word, J. M., Prisant, M. G., Richardson, J. S. & Richardson, D. C. (2002). *Proteins Struct. Funct. Genet.* **50**, 437–450.
Luft, J. R., Collins, R. J., Fehrman, N. A., Lauricella, A. M., Veatch, C. K. & DeTitta, G. T. (2003). *J. Struct. Biol.* **142**, 170–179.
McPhillips, T. M., McPhillips, S. E., Chiu, H.-J., Cohen, A. E., Deacon, A. M., Ellis, P. J., Garman, E., Gonzalez, A., Sauter, N. K., Phizackerley, R. P., Soltis, S. M. & Kuhn, P. (2002). *J. Synchrotron Rad.* **9**, 401–406.
Merritt, E. A. & Hol, W. G. J. (1995). *Curr. Opin. Struct. Biol.* **5**, 165–171.
Minke, W. E., Pickens, J., Merritt, E. A., Fan, E., Verlinde, C. L. M. J. & Hol, W. G. J. (2000). *Acta Cryst.* D**56**, 795–804.
Murshudov, G. N., Skubák, P., Lebedev, A. A., Pannu, N. S., Steiner, R. A., Nicholls, R. A., Winn, M. D., Long, F. & Vagin, A. A. (2011). *Acta Cryst.* D**67**, 355–367.
Nawar, H. F., Arce, S., Russell, M. W. & Connell, T. D. (2005). *Infect. Immun.* **73**, 1330–1342.
Nawar, H. F., Berenson, C. S., Hajishengallis, G., Takematsu, H., Mandell, L., Clare, R. L. & Connell, T. D. (2010). *Clin. Vaccine Immunol.* **17**, 969–978.
Ohto, U., Fukase, K., Miyake, K. & Satow, Y. (2007). *Science*, **316**, 1632–1634.

Park, B. S., Song, D. H., Kim, H. M., Choi, B.-S., Lee, H. & Lee, J.-O. (2009). *Nature (London)*, **458**, 1191–1195.
Pickens, J. C., Merritt, E. A., Ahn, M., Verlinde, C. L., Hol, W. G. J. & Fan, E. (2002). *Chem. Biol.* **9**, 215–224.
Sonnino, S., Acquotti, D., Riboni, L., Giuliani, A., Kirschner, G. & Tettamanti, G. (1986). *Chem. Phys. Lipids*, **42**, 3–26.
Vagin, A. & Teplyakov, A. (2010). *Acta Cryst.* D**66**, 22–25.
Winn, M. D. *et al.* (2011). *Acta Cryst.* D**67**, 235–242.